Experimental and clinical investigation of efficiency and ablation profiles of new solid-state deep-ultraviolet laser for vision correction

Anna M. Roszkowska, MD, PhD, Georg Korn, PhD, Matthias Lenzner, PhD, Marcel Kirsch, Olaf Kittelmann, PhD, Rafal Zatonski, Paolo Ferreri, MD, Giuseppe Ferreri, MD

Purpose: To investigate the efficiency and ablation profiles of a newly developed, all-solid-state laser platform.

Setting: Experimental investigations performed at Katana Technologies GmbH, Kleinmachnow, Germany, and clinical study, at the Ophthalmology Clinic, University of Messina, Messina, Italy.

Methods: Experimental studies were performed on poly(methyl methacrylate) (PMMA) and in porcine eyes using an all-solid-state, Q-switched, frequency-shifted laser (LaserSoft, Katana Technologies GmbH) with a Gaussian spot with a diameter of 0.2 mm in the target plane, a peak fluence of 350 mJ/cm^2, and a repetition rate of 1 kHz. The ablation profiles were determined using a profile meter (MicroProf, Fries Research and Technology GmbH), corneal topography was analyzed with a TMS 2N (Tomey Inc.), and corneal thickness was measured with an ultrasound pachymeter (DGH Technology). In the clinical study, 9 human eyes were treated with photorefractive keratectomy. The mean outcome measures were uncorrected visual acuity (UCVA), best spectacle-corrected visual acuity (BSCVA), corneal topography, and corneal transparency. The follow-up was 1 month for all eyes and 3 months for 4 eyes. Safety, efficacy, and predictability were evaluated.

Results: Smooth profiles were found in the PMMA and the porcine eyes. The topographic maps showed central steepening after the hyperopic ablation and slight central flattening of the surface after the myopic treatment. No eye lost lines of BSCVA; the UCVA improved in all eyes. All eyes were within ±1.00 diopter (D) of emmetropia, and 89% were within ±0.50 D.

Conclusion: The efficacy of the ablation was good, with the profile meter results confirmed by the topographic measurements.

J Cataract Refract Surg 2004; 30:2536–2542 © 2004 ASCRS and ESCRS

Over the past years, laser vision correction has been successfully performed using excimer lasers as ultraviolet (UV) sources.[1] During the past 10 years, solid-state lasers have improved and become a reliable source for treating organic and inorganic tissue materials.[2–7] Their advantage is a considerable reduction of the problems associated with excimer lasers, permitting high pulse-to-pulse stability, a smaller spot size, and a higher repetition rate. Because of the absence of a gas, the maintenance costs are lower; because of the lack of a gas discharge, the noise level during operation of the laser is significantly lower.

Earlier solid-state devices had a gas discharge in the flash lamps used to pump the solid-state laser material. With the emergence of powerful laser diodes, the flash lamps have been replaced, eliminating the last drawback of solid-state systems. For this reason, the state-of-the-art systems are denoted as "all-solid-state."

In these devices, a continuously operating laser diode bar pumps a neodymium-doped:YLF crystal,

0886-3350/04/$–see front matter
doi:10.1016/j.jcrs.2004.04.071

which is enclosed, into a laser cavity. Intracavity harmonic generation and periodic modulation of the cavity loss lead to an extremely stable train of Q-switched green (527 nm) pulses with a repetition rate of 1 kHz or higher and single-pulse duration of about 100 nanoseconds. Unlike an excimer laser that provides the inversion (gain) due to the build up of an excited dimer in a pulsed gas discharge, this laser maintains the gain permanently due to its highly stable continuous-wave diode pumping. The periodic modulation then generates the necessary giant pulse with the required repetition rate. This leads to a higher level of stability for the generated pulse trains than with lamp-pumped Q-switched lasers. The measured stability is better than 1% (root-mean-square) for this laser.

In the LaserSoft device (Katana Technologies GmbH), the pulses are used to pump a titanium-doped sapphire laser in a second resonator, in which a wavelength of 840 nm, a small bandwidth, and pulse duration of about 10 nanoseconds are achieved by several means. New technology (patent pending) enables stability of the wavelength, pulse duration, and pulse energy of the emerging pulse train. Subsequently, the wavelength of these pulses is bisected twice in 2 nonlinear crystals. Saturating 1 of the frequency doublings offsets the increase in instability that is inherent in nonlinear processes.

At the end of this chain, 210 nm pulses with a duration of about 8 nanoseconds and the unaltered repetition rate of 1 kHz are delivered to the target. The spatial distribution is Gaussian with a beam diameter (full width at half maximum) of 150 μm; due to the last nonlinear process, the shot-to-shot stability declines to 2.8% (standard deviation) in the UV. The fluence can be continuously adjusted up to 400 mJ/cm^2.

In this study, experimental and clinical ablations were performed using this newly developed small-spot-size, high-repetition-rate, all-solid-state laser. The potential of the laser for customized ablation is reported.

Materials and Methods

Ablation profiles equivalent to myopic, hyperopic, and astigmatic corrections were generated in poly(methyl methacrylate) (PMMA) and in porcine eyes. The beam diameter, D, of 200 μm is taken at the 1/e level (37%) of the peak fluence, F_O ($F_O = 4\ E/\pi D^2$, where E is the laser pulse energy). The experiments were performed with a peak fluence of 350 mJ/cm^2, resulting in a maximum ablated volume for the given diameter and material threshold fluence (50 mJ/cm^2). Existing reports state that corneal ablation rates at a 213 nm wavelength (quintupled neodymium:YAG laser) are comparable to those of excimer lasers at 193 nm for similar repetition rates and pulse duration.[4–7]

The placement of single laser pulses on the target is computed by adding single-shot ablation profiles, generated by these pulses, until the desired ablation profile is achieved. The generated data are converted to control 2 scanning mirrors, which direct each laser pulse to its calculated position. This produces smooth ablation profiles equivalent to corrections of myopia, hyperopia, and astigmatism. The device is equipped with a continuously working eye tracker exhibiting a latency time of 1 millisecond.

To evaluate the performance of the system, the resulting ablation profiles were measured and single-shot ablation rates and profiles deduced. In PMMA and in porcine eyes, a noncontact optical profiling system (MicroProf® detector, Fries Research and Technology GmbH) was used. With a depth resolution of 300 nm and a viewing field of 7.0 mm × 7.0 mm, this device permits fast, noninvasive, and precise measurement of ablated surfaces.

In a second set of experiments, fresh pig eyes were treated. The epithelium was removed mechanically, and the eyes were fixed on a specially prepared support that allowed stable and reproducible positioning of the eye to the superior, inferior, temporal, and nasal sides. The corneal maps were taken with a topographic modeling system (TMS 2N, Tomey Inc.). A 0.9% physiological solution was used to improve the corneal surface and to permit sufficient reflection for good acquisition of the images. The corneal thickness was measured before and after ablation with an ultrasound pachymeter (DGH Technology), and these data were used to determine the effective ablation depth. The

Accepted for publication April 6, 2004.

From the Ophthalmology Clinic, University of Messina (Roszkowska, P. Ferreri, G. Ferreri), Messina, Italy, and Katana Technologies GmbH (Korn, Lenzner, Kirsch, Kittelmann, Zatonski), Kleinmachnow, Germany.

Presented in part at the XXIst Congress of the European Society of Cataract & Refractive Surgeons, Munich, Germany, September 2003.

Drs. G. Ferreri and Roszkowska are consultants to Katana Technologies GmbH. Drs. Korn, Lenzner, Kittlemann and M. Kirsch and R. Zatonski are employed by Katana. Dr. P. Ferreri has no financial or proprietary interest in any product mentioned.

Reprint requests to Dr. A.M. Roszkowska, Ophthalmology Clinic, Policlinico Universitario, Via Consolare Valeria, 98100 Messina – Gazzi, Italy. E-mail: anrosz@tiscali.it.

eyes with the best corneal profiles were chosen for the ablation experiments.

In the clinical investigation, the refractive procedure was performed in 9 human eyes. Four eyes had myopia, 3 eyes had compound myopic astigmatism, and 2 eyes had compound hyperopic astigmatism. The preoperative assessment included uncorrected visual acuity (UCVA), best spectacle-corrected visual acuity (BSCVA), tonometry, corneal topography, pachymetry, refractometry, cycloplegic refraction, retinoscopy, pupillometry, Schirmer test, and endothelial microscopy. Exclusion criteria were change in refraction within the last year, corneal pathology, glaucoma, and systemic diseases such as diabetes and immunology disorders.

Informed consent was obtained from all patients, and photorefractive keratectomy was performed by 2 surgeons (A.R., G.F.). The ablation zone varied from 6.5 to 7.0 mm for the treatment of myopia and myopic astigmatism and from 6.0 to 9.0 for compound hyperopic astigmatism. A soft contact lens was applied after the treatment, and all patients received drops of antibiotic agents, nonsteroidal antiinflammatory agents, and artificial tears 4 times daily until epithelium healing was complete and the contact lenses were removed. After this, the patients were given corticosteroid drops 3 times daily.

The main outcome measures were UCVA, BSCVA, corneal topography, and transparency. The follow-up examination was 1 month for all eyes and 3 months for 4 eyes.

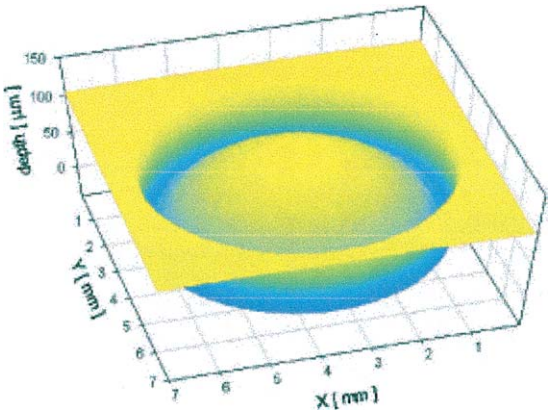

Figure 1. (Roszkowska) Three-dimensional view of PMMA surface treated for hyperopia.

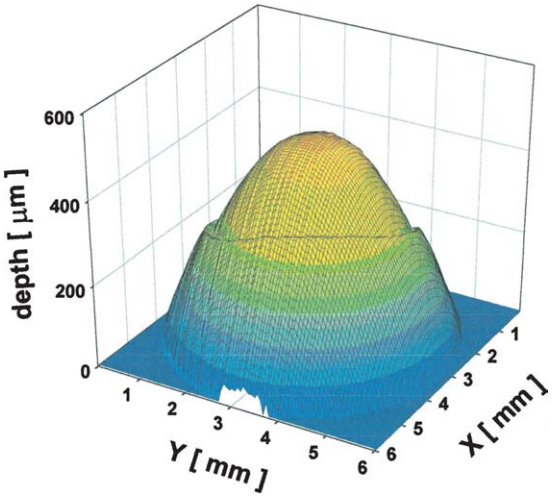

Figure 2. (Roszkowska) Three-dimensional view of a porcine cornea after hyperopic treatment of +6.0 D with an ablation zone of 4.0 mm.

Results

Experimental Studies

Figure 1 shows a measured ablated PMMA surface representing a hyperopic correction with an ablation zone diameter of 6.0 mm.

Figure 2 shows the surface of a pig eye after an ablation corresponding to a hyperopic treatment of +6.0 D with an ablation zone diameter of 4.0 mm measured with the optical profiler. In this case, a transition zone was not ablated to enable visualization of the step at the edge of the ablation zone that is typical in a hyperopic treatment. Although a steep central island was not observed in the ablation experiments, treatments that simulated its removal were performed to demonstrate the abilities of the new laser system to finely structure the cornea. For this purpose, an additional myopic correction of −6.0 D with an optical zone of 2.0 mm was ablated on top of the hyperopic correction. Slight flattening of the surface can be seen in Figure 3, which corresponds to removal of a steep central island with an optical power of +6.0 D.

In another porcine eye, the 2-step treatment described above was repeated. At first, a hyperopic correction of +6.0 D with a diameter of 4.0 mm was ablated. The corneal topography performed immediately afterward exhibited central steepening of approximately 8.5 D (Figure 4). A myopic correction of −6.0 D with a 2.0 mm diameter was ablated on top of the steepening. The resulting corneal map shows central flattening with a magnitude of approximately 8.0 D, almost restoring the original corneal curvature (Figure 5). The accuracy of this measurement was influenced by the fact that the enucleated pig eyes were

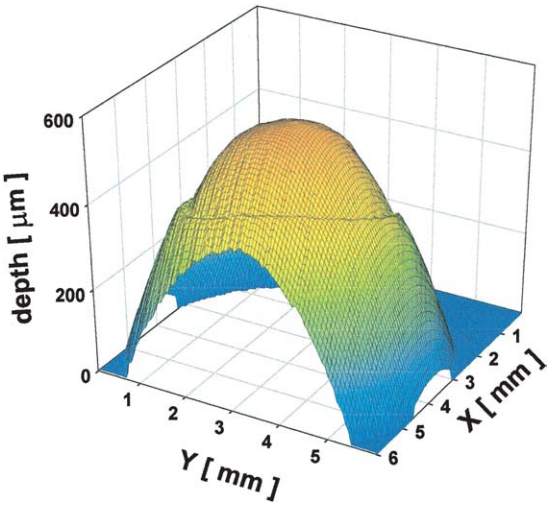

Figure 3. (Roszkowska) Three-dimensional view of an additional myopic treatment of −6.0 D with an ablation zone of 2.0 mm on top of the hyperopic ablation shown in Figure 2. This corresponds to removal of a steep central island with a diameter of 2.0 mm and an optical power of +6.0 D.

mounted on a special holder and moved from the horizontal (ablation position) to the vertical position (topographic measurement).

A further step in the clinical investigation was determining the achieved versus intended ablation depths in pig eyes. Table 1 shows the measured ablation depths for different corrections of myopia and phototherapeutic keratectomy. The difference between the predicted and the achieved values was equal to or less than 10%.

Clinical Study

The preoperative UCVA was 20/100 or less in 5 eyes, 20/50 in 3 eyes, and 20/40 in 1 eye. At 1 month, the UCVA was 20/25 or better in all eyes; it was 20/20 or better in 7 of the eyes. The preoperative BSCVA was 20/25 in 1 eye and 20/20 or better in 8 eyes. At 1 month, no eye lost a line of BSCVA and 3 eyes gained 1 line. The mean preoperative SE was −2.28 D (range −7.63 to +1.50 D); at 1 month, it was −0.17 D (range −0.50 to emmetropia). At 1 month, 100% of eyes were within ±1.00 D of emmetropia, 89% were within ±0.50 D, and 67% within ±0.25 D.

At the 3-month follow-up in 4 eyes, the UCVA was 20/20 or better in 3 eyes and 20/25 in 1 eye. The BSCVA did not change from the 1-month BSCVA in 3 eyes; it improved in 1 eye. The SE refraction was −0.88 D in 1 eye; 3 eyes were emmetropic. Table 2 shows the refractive outcome in the treated patients.

The corneal maps showed a smooth, regular pattern with wide ablation zones; all treatments were well centered (Figures 6 to 8).

Complete reepithelialization was achieved within 3 to 5 days of treatment. Good corneal transparency was observed during the entire follow-up (Figure 9).

Discussion

Customized corneal ablation in laser vision correction requires the ablation of a predetermined profile, which is increasingly sophisticated if higher-order

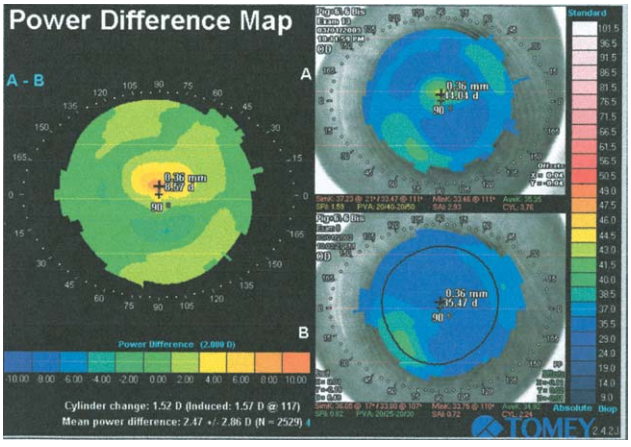

Figure 4. (Roszkowska) Power difference map of a porcine cornea treated for +6.0 D hyperopia with an ablation zone of 4.0 mm. The difference map shows regular central steepening of approximately 8.5 D. The pretreatment regular profile is shown in the inferior map and the postablation pattern, in the superior map.

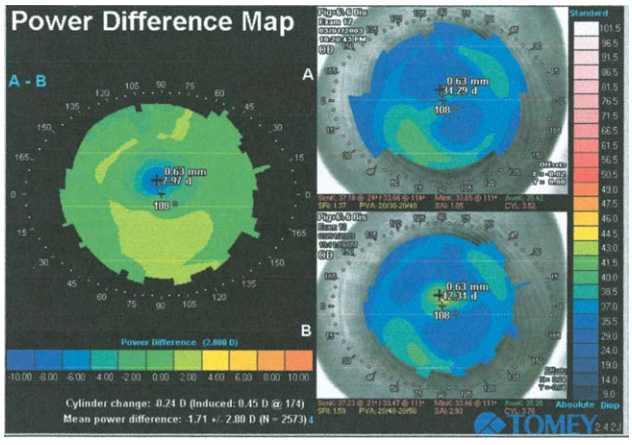

Figure 5. (Roszkowska) The difference map of a myopic treatment on top of previous central hyperopic steepening. The −0.6 D treatment had an ablation zone of 2.0 mm. The small central flattening of approximately 8.0 D is evident and located exactly on the previous central steepening.

Table 1. Measured ablation depth for various corrections of myopia and PTK.

Sample (Pig Eyes)	Treatment OZ/TZ (mm)	Maximum Depth Predicted (μm)	Pachymetry After Removal of Epithelium (μm)	Pachymetry After Treatment (μm)	Difference (μm)	Deviation (%)
1	Sph −10.0 D 6.5/8.5	148	740	600	140	−5.7
2	Sph −8.0 D 7.0/9.0	144	735	594	141	−2.1
3	PTK 100 μm 4.0	100	770	680	90	−10.0

OZ = optical zone; PTK = phototherapeutic keratectomy; Sph = sphere; TZ = transition zone

abberations are to be corrected. The high resolution necessary for this goal can be achieved only with rather small spot sizes on the target and smooth fluence distributions over the spot area. With a scanning-spot laser, the estimated spot size necessary for an 8th-order (Zernike term) correction is less than 0.5 mm for an optical zone diameter of 6.0 mm.[6] Taking into account the results of wavefront measurements of the aberrated eye, wavefront-guided customization can be achieved.[6]

The newly developed device investigated in this study provides a spot diameter of 0.2 mm (at the 1/e value of F_O) and an ablation zone variable up to 10.0 mm. These characteristics allow a precise customized ablation. In our experiments, the removal of a steep central island with an optical power of +6.0 D yielded promising results. The maximum elevation of the cornea for such a steep central island would be 8.0 μm. Such a precise treatment is impossible with a laser spot size of 1.0 mm or more.

Another important aspect of the small spot diameter is the smaller mechanical stress caused by the acoustic shock wave that is generated by the ablation process. Krueger et al.[7] measured these acoustic shock waves and concluded that their amplitude increases as the spot diameter increases. Kermani and Lubatschowski[8] assumed that the mechanical stress involved in laser-induced acoustic shock waves might produce cellular alterations that damage the collagen structure.

With the studied device, the high repetition rate (1 kHz) and the low energy per pulse resulted in a completely quiet treatment. No audible acoustic waves, such as those during excimer laser treatments, were generated.

The accuracy of the achieved profiles, the small spot size, and the high pulse-to-pulse stability make this solid-state laser platform a good choice for customized corneal ablation and an alternative to

Table 2. The refractive outcome in treated patients.

	Preoperative						1 Month Postop					
Eye	UCVA	BSCVA	Sph	Cyl	Axis	SE	UCVA	BSCVA	Sph	Cyl	Axis	SE
1	<0/200	20/25	−7.00	−1.00	160	−7.50	20/25	20/25	0.00	−0.75	165.00	−0.38
2	<20/200	20/20	−7.00	−1.25	90	−7.63	>20/20	>20/20	0.00	0.00	—	0.00
3	20/50	20/20	1.00	1.00	180	1.50	20/20	20/20	−0.50	0.00	—	−0.50
4	20/50	20/20	1.00	0.75	180	1.38	>20/20	>20/20	0.00	0.00	—	0.00
5	20/100	>20/20	−1.75	0.00		−1.75	>20/20	>20/20	0.00	0.00	—	0.00
6	20/40	>20/20	−1.25	0.00		−1.25	>20/20	>20/20	0.00	0.00	—	0.00
7	20/100	20/20	−1.25	−1.00	10	−1.75	>20/20	>20/20	0.00	0.00	—	0.00
8	20/50	>20/20	−1.50	0.00		−1.50	20/20	>20/20	−0.50	0.00	—	0.00
9	<20/200	20/20	−2.75	0.00		−2.75	20/25	20/20	−0.50	−0.50	5.00	−0.75

BSCVA = best spectacle-corrected visual acuity; Cyl = cylinder; SE = spherical equivalent; Sph = sphere; UCVA = uncorrected visual acuity

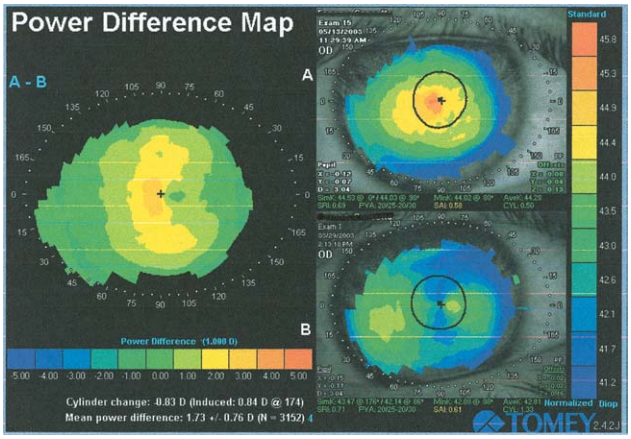

Figure 6. (Roszkowska) Corneal topography of compound hyperopic astigmatism treatment.

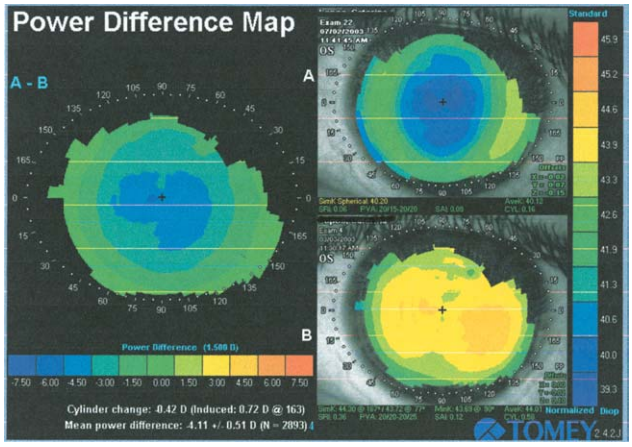

Figure 7. (Roszkowska) Corneal topography of compound myopic astigmatism ablation.

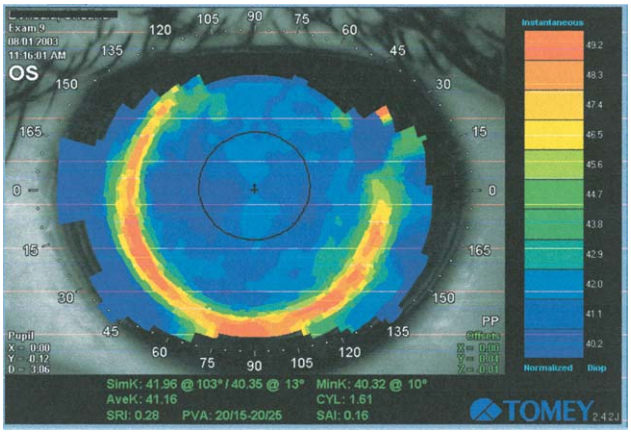

Figure 8. (Roszkowska) Corneal topography after −6.0 D myopic treatment. The wide ablation zone is visible.

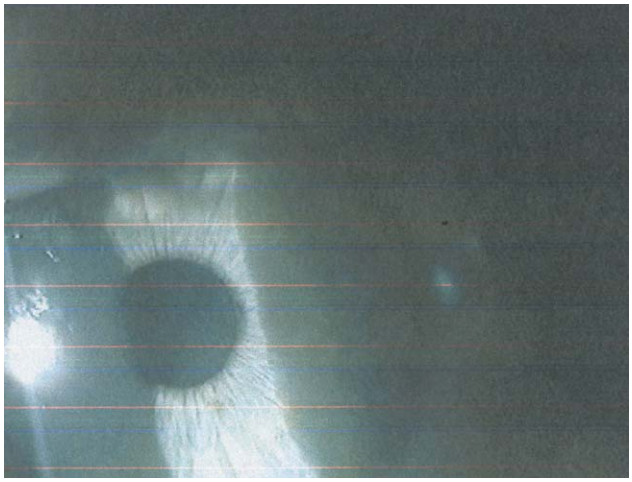

Figure 9. (Roszkowska) Corneal transparency 3 months after treatment.

Table 2 (cont.)

3 Months Postop					
UCVA	BSCVA	Sph	Cyl	Axis	SE
20/25	20/20	−0.50	−0.75	165	−0.88
>20/20	>20/20	0.00	0.00	—	0.00
20/20	20/20	0.00	0.00	—	0.00
>20/20	>20/20	0.00	0.00	—	0.00
—	—	—	—	—	—
—	—	—	—	—	—
—	—	—	—	—	—
—	—	—	—	—	—
—	—	—	—	—	—

fluorine-based excimer lasers for the correction of refractive errors. The primary results are good precision and reproducibility, smooth surfaces, and convenient handling. The profile meter results were confirmed by topographic measurements after ablation.

The clinical results showed high efficacy, with all eyes within ±1.0 D of the intended correction and 89% of eyes within ±0.50 D. That no lines of BSCVA were lost confirms the safety of the treatment. The stability of the results should be investigated further, although the stability of the results in 4 eyes was confirmed at the 3-month follow-up. The clinical results should be investigated in a larger number of eyes with adequate follow-up.

Conclusions

The characteristics of the new solid-state laser are a small spot diameter with true Gaussian intensity distribution, a high repetition rate, and silent operation. The beam profile induces a smooth surface after treatment and smooth and well-defined transition zones and allows customized ablation with high precision. Less energy per pulse is applied to the corneal surface and therefore less corneal scarring should be expected. The solid-state approach reduces the requirements for maintenance and the related costs, and the diode pumping system features long lifetime and efficiency. These characteristics make LaserSoft a safe, stable, more compact, and less costly alternative than gas-operating excimer lasers for refractive surgery.

References

1. Munnerlyn CR, Koons SJ, Marshall J. Photorefractive keratectomy: a technique for laser refractive surgery. J Cataract Refract Surg 1988; 14:46–52
2. Dair GT, Pelouch WS, van Saarloos PP, et al. Investigation of corneal ablation efficiency using ultraviolet 213-nm solid state laser pulses. Invest Ophthalmol Vis Sci 1999; 40:2752–2756
3. Gailitis RP, Ren QS, Thompson KP, et al. Solid state ultraviolet laser (213 nm) ablation of the cornea and synthetic collagen lenticules. Laser Surg Med 1991; 11:556–562
4. Ren Q, Simon G, Parel J-M. Ultraviolet solid-state laser (213-nm) photorefractive keratectomy; in vitro study. Ophthalmology 1993; 100:1828–1834
5. Ren Q, Simon G, Legeais J-M, et al. Ultraviolet solid-state laser (213-nm) photorefractive keratectomy; in vivo study. Ophthalmology 1994; 101:883–889
6. MacRae SM, Krueger RR, Applegate RA, eds. Customized Corneal Ablation; the Quest for SuperVision. Thorofare, NJ, Slack, 2001
7. Krueger RR, Seiler T, Gruchman T, et al. Stress wave amplitudes during laser surgery of the cornea. Ophthalmology 2001; 108:1070–1074
8. Kermani O, Lubatschowski H. Struktur und Dynamik photoakustischer Shockwellen bei der 193 nm Excimerlaserphotoablation der Hornhaut. Fortschr Ophthalmol 1991; 88:748–753